Acta Zoologica

Published for The Royal Swedish Academy of Sciences and The Royal Danish Academy of Sciences and Letters

Acta Zoologica (Stockholm) doi: 10.1111/azo.12007

Skeletogenesis in anurans: cranial and postcranial development in metamorphic and postmetamorphic stages of *Leptodactylus bufonius* (Anura: Leptodactylidae)

Miriam Corina Vera[1] and María Laura Ponssa[2]

[1]Fac. de Ciencias Nat. e Inst. Miguel Lillo, Univ. Nacional de Tucumán, Instituto de Herpetología, Fundación Miguel Lillo, Miguel Lillo 251, San Miguel de Tucumán (4000), Argentina; [2]CONICET, Instituto de Herpetología, Fundación Miguel Lillo, Miguel Lillo 251, San Miguel de Tucumán (4000), Argentina

Keywords:
juvenile, skeletal development, skull-shape change, anuran, *Leptodactylus*

Accepted for publication:
2 October 2012

Abstract

Vera, M.C. and Ponssa, M.L. 2013. Skeletogenesis in anurans: cranial and postcranial development in metamorphic and postmetamorphic stages of *Leptodactylus bufonius* (Anura: Leptodactylidae). — *Acta Zoologica* (Stockholm) **00**: 000–000.

Osteological studies of anurans generally have focused on the descriptions of adults and larval chondrocrania, including developmental series of chondrocrania. Thus, the changes occurring during postmetamorphic stages have largely been overlooked. Herein, we describe cranial and postcranial skeletogenesis, and change in skull shape through the metamorphic and postmetamorphic development of *Leptodactylus bufonius*. Several elements, particularly those of the cranium, are already ossified at metamorphic climax; among these elements are the frontoparietals, prootics, premaxillae, maxillae, squamosals, pterygoids, neopalatines, angulosplenials, dentaries, mentomeckelians, and the mesosternum. Determining the exact timing of ossification of some elements is difficult because variation in their development may result from extrinsic factors. The otic region and that of the jaw closure undergo the greatest changes in shape, which may imply functional constraints. The development of many skeletal elements is still incomplete at metamorphosis; thus, the changes occurring postmetamorphically are crucial to achieving the configuration and function of an adult skeleton.
María Laura Ponssa. CONICET. Instituto de Herpetología, Fundación Miguel Lillo. S. M. de Tucumán, c/p (4000), Argentina. E-mail: mlponssa@hotmail.com.

María Laura Ponssa, CONICET, Instituto de Herpetología, Fundación Miguel Lillo, Miguel Lillo 251, San Miguel de Tucumán (4000), Argentina.
E-mail: mlponssa@hotmail.com

Introduction

Studies of the anatomical skeletal complexity and development in vertebrates provide information on morphological and functional diversification (e.g., Cardini 2003; Cardini and O'Higgins 2005; Mitteroecker *et al.* 2005). However, these generalizations are not especially evident in anurans, because typically, frogs and toads undergo significant structural changes during metamorphosis (Ivanović *et al.* 2007). To gain a perspective of the evolutionary changes in amphibian skeletal ontogeny and the consequences of a biphasic lifestyle, it is necessary to study the patterns of variation during ontogeny (Ivanović *et al.* 2007). Since the early work of Ecker (1889) on the anatomy of *Pelophylax ridibundus* (*Rana esculenta*), studies of anurans have focused on the descriptions of adults, larval chondrocrania, and developmental series of chondrocrania (e.g., Trueb 1985; de Sá 1988; Wiens 1989; de Sá and Trueb 1991; de Sá and Lavilla 1996; Púgener and Maglia 1997; Wild 1997; Maglia and Púgener 1998; Trueb *et al.* 2000; Perotti 2001; Ponssa 2006; Ponssa and Heyer 2007; Vera Candioti *et al.* 2007). Although there is abundant literature on the development of the anuran chondrocranium,

the development of the osteocranium largely has been overlooked (Trueb 1985). This is surprising because the configuration that corresponds to the adult morphology is determined throughout the postmetamorphic stages of the life cycle (Duellman and Trueb 1986; Djorović and Kalezić 2000; Lebedkina 2004).

Leptodactylus comprises 89 species (Frost 2011). One of the characteristics of *L. bufonius*, which is a member of the *L. fuscus* Group, is that males construct nuptial chambers for the construction of the foam nest and deposition of the eggs. The first larval stages develop in chambers of the foam nest (Pisano *et al.* 1993; Reading and Jofré 2003). *Leptodactylus bufonius* is a sister species of *L. troglodytes*; both are characterized by having a tectum nasi that bears an anterior prenasal process (Ponssa 2008). The larval and adult skeletons of *L. bufonius* and its congeners have been the focus of several studies (Larson and de Sá 1998; Ponssa 2006, 2008; Ponssa and Heyer 2007; de Sá *et al.* 2007; Vera Candioti *et al.* 2007; Ponssa *et al.* 2010b, 2011); however, significant cranial changes that characterize the transition from the metamorphic to the adult frog are unknown. Herein, we describe the skeletal development and the changes in skull shape throughout the metamorphic and postmetamorphic stages of *Leptodactylus bufonius*; we also compare our observations with the available information on other anurans species. Our objective is to provide baseline descriptive data to test the hypothesis that a metamorphic frog is not simply a small copy of an adult, and that through the postmetamorphic development, significant events occur to allow the frog to face the functional challenges of adult life.

Materials and Methods

A total of 35 specimens of *Leptodactylus bufonius* from the herpetological collection of Instituto de Herpetología of Fundación Miguel Lillo, Tucumán, Argentina, were examined. Specimens are identified as follows: FML 00256/10,00256/76, 00256/126, 00256/148, 00256/160, 00256/202, 00256/235, 00256/246, 00256/249, 00256/266, 00587/5, 00587/6, 00589, 00672 (A), 00672 (B), 03568 (A), 03568 (B), 04908 (A), 04908(B), 04908(C), 08010, 08011, 09780, 09779, 12129, 12130, 12132, 12133, 12134, 12135, 12136, 12137, 12138, 12139, 12144. The ontogenetic stages analyzed were metamorphs between Gosner (1960) Stages 43 and 46, and juvenile postmetamorphs, which were ordered according to their snout–vent length; 21 juvenile stages were recognized. The juvenile frogs are identified easily with the external characters provided by Heyer (1978). Only the white tubercles in the sole of the foot, which are present in *L. troglodytes* and absent in *L. bufonius,* are not readily apparent in juveniles. However, the specimens were unequivocally assigned to *L. bufonius* because of their Chacoan distribution, in contrast to *L. troglodytes* that occurs in NE Brazil (Heyer 1978).

Each postmetamorphic specimen was measured with digital calipers (Mitutoyo CD-30C and CD-15B; ±0.01 mm) and a stereoscopic Karl Zeiss Discovery V.8 microscope equipped with an ocular micrometer. The measurements were taken as follows: snout–vent length; cranium length and width; femur, tibia, tarsus and pes length; tympanum diameter; and inter-nostril distance (Table 1). Adult frogs were used to compare the osteology of the limbs and analyze the changes of some structures, such as sesamoids, short bones, and epiphyses. Specimens were cleared and double-stained for bone and cartilage with Alizarin red and Alcian blue following Wassersug's technique (1976). Cartilaginous structures stained with Alcian blue, whereas calcium associated with mineralization and ossification stained red with Alizarin Red S. Mineralization was indicated by diffuse, irregular spots in a cartilaginous matrix, whereas ossification was indicated by uniformly red-stained bone. Clearing and double-staining can result in variable color patterns resulting from different preservation techniques. Although the same collecting and preservation protocols were used for all of our samples, it is important to note that specimens used in other studies may appear different than ours. The skull morphology of juveniles was compared with the description of adult *Leptodactylus* skull (Ponssa 2008). The terminology for cranial and postcranial osteology follows that of Trueb (1973, 1993) and Trueb *et al.* (2000); both digital and carpal osteology follows that of Fabrezi (1992); laryngeal morphology is that of Trewavas (1933); and sesamoid terminology that of Ponssa *et al.* (2010a). Fingers are numbered II–V following Fabrezi and Alberch (1996). Observations and illustrations were made using Zeiss Discovery. V8 stereoscope with an attached camera lucida and with a Nikon Coolpix P60005-megapixel digital camera.

Thin-plate spline (TPS) morphometric analyses were conducted to describe shape changes associated with ontogenetic growth in postmetamorphs of *Leptodactylus bufonius*. Images of the skulls in dorsal and ventral views of 12 specimens chosen to represent different stages of postmetamorphic growth were recorded with a Nikon Coolpix P6000 digital camera. Specimens with digits corresponding to Gosner (1960) Stage 46, juvenile Stages 0, 2, 4, 5, 6, 8, 9, 13, 17, 21 and adult. TPS methods are used to describe shape changes with a set of landmark data independent of size, location, or orientation (Bookstein 1991). One of us (M.C.V.) digitized 21 dorsal and 24 ventral landmarks, and three ventral semi-landmarks with TpsDig ver. 2.16 software (Rohlf 2010) on the right half of each skull image (Fig. 1; landmarks and semi-landmarks defined in caption). A landmark usually represents the most distal tip of a corner of a process, an intersection of tissues, or point of maximum curvature of structures (Bookstein 1991), whereas a semi-landmark refers to a point located anywhere between two mathematical or anatomical landmarks (Dryden and Mardia 1998). We selected the landmarks and semi-landmarks based on their ease of identification in all specimens and their utility in representing the entire geometric form and in providing functional descriptions of important regions of the skull

Table 1 Measurements of metamorph (according to Gosner 1960) and juveniles stages of *Leptodactylus bufonius*

Stages	SVL	HL	HW	TL	SL	TTL	FL	TD	IN
43	23.13	10.86	8.7	8.64	9.35	6.29	10.4	–	2.27
43	22.97	9.44	7.86	10.06	8.22	5.21	10.37	–	2.65
46	10.9	4.13	3.74	4.8	5.68	2.99	5.37	–	1.47
0	12.49	5.25	4.04	5.19	6.21	3.49	6.49	–	1.77
1	12.6	5.22	4.6	5.53	6.3	3.58	6.52	–	1.16
2	13.94	5.45	4.92	5.51	6.26	3.18	5.87	–	1.69
3	14.15	5.51	4.47	5.63	7.03	3.76	6.98	–	1.21
4	15.38	5.48	5.27	6.35	7.13	3.73	7.55	–	1.71
5	16.68	7.69	6.26	7.24	8.62	4.99	8	1.06	1.61
6	18.79	7.42	7	8.15	8.99	4.72	9.3	1.56	2.2
7	21.11	8.5	6.82	7.95	10.36	5.68	10.64	1.28	2.23
8	21.3	8.66	7.49	9.45	10.42	5.25	10.4	1.77	2.1
9	23.5	10.09	8.57	9.21	10.08	5.93	11.41	1.82	2.54
10	23.56	8.39	7.51	9.36	9.64	5.45	10.76	1.93	2.65
11	24.23	9.99	8.86	8.97	9.76	5.33	12.05	1.43	2,32
12	25.8	9.89	9.52	10.29	12	6.31	12.53	1.87	2.53
13	26.13	11.3	9.04	10.22	11.08	6.94	12.01	1.85	2.67
14	27.37	10.19	9.1	11.04	11.41	6.89	12.82	1.25	3.02
15	28.55	12.19	10.1	11.1	11.58	6.57	13.01	1.98	2.89
16	28.97	11.57	10.48	11.56	12.87	6.37	12.68	1.83	2.6
17	31.79	12.49	11.5	12.08	13.69	8.02	13.63	2.5	2.7
18	32.74	12.21	11.85	13.58	13.73	7.9	13.85	2.73	3.21
19	34.97	14.44	12.78	13.61	15.42	8.76	15.24	2.73	3.13
20	36.63	15.15	13.05	13.95	16.24	8.9	15.79	3.21	3.39
21	37.72	15.73	13.87	14.13	15.79	8.6	15.17	2.94	3.4

SVL, snout–vent length; HL, head length; HW, head width; TL, thigh length; SL, shank length; TTL, tibiale–tarsale length; FL, foot length; TD, greatest tympanum diameter; IN, inter-nostril distance.

(Larson 2002). For the ventral configuration of the skull, two analyses were performed: one included all the stages indicated above (Stages 46–adult), not including the landmarks corresponding to the dentigerous process of the vomer (landmarks 25, 27; semi-landmark 26), and the other analysis excluded the first postmetamorphic stages and included the landmarks corresponding to the dentigerous process of the vomer. It was necessary to perform both the analyses, because in early stages, the dentigerous process of vomer is absent. For each specimen, decomposition of shape into orthogonal principal warps provides a set of principal-warp coefficients that describe deviation of the specimen from a generalized orthogonal least-square Procrustes consensus configuration. Relative warp (RW) analyses are derived from a principal component analysis of the principal-warp coefficients and permit the description of the primary axes along which the shape changes occur (Bookstein 1991). RW analyses were conducted to study the dorsal and ventral views of the skull using TPS relw 1.37(Rohlf 2003).

Results

Individual growth is reflected in the measurements of the skeletal elements (Table 1). The sequential order of ossification of cranial and postcranial elements is shown in Table 2. Hanken and Hall (1988) observed that ossification can be detected in sectioned specimens in several Gosner stages before it is visible in cleared-and-stained whole-mount preparations; thus, the results presented here should be considered estimates of ossification timing.

Cranium

Sphenethmoid. The sphenethmoid is cartilaginous in Stage 43 and from Stages 9–16. In Stages 46, 0, 1, 5–8, and 17–21, the endochondral ossification is a round center on each side of the braincase. In Stages 2–4, the sphenethmoid ossification is visible in ventral and dorsal views. In the smallest specimens examined (Stages 43, 46, and 0–6), the lateral margin of this element lies on the anterior fifth of the orbit (Fig. 2).

Exoccipital. The exoccipital is mineralized in metamorphic specimens (Stages 43 and 46); in Stages 0–8, it is ossified, with only the end of the occipital condyle remaining cartilaginous. The bone is ossified in Stages 9–21. In the specimens examined, the exoccipitals are not fused with the prootics.

Prootic. The prootics form the posterolateral of the braincase, and the dorsal, anterior, and lateral walls of the otic capsules. The prootics are mineralized in metamorphic stages (43 and

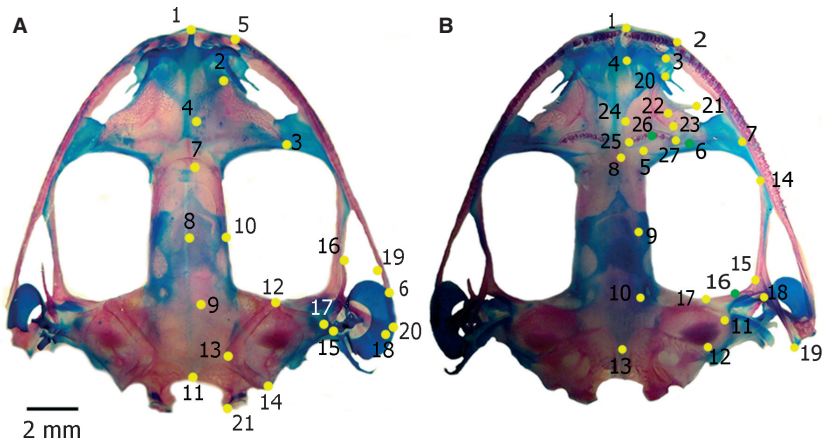

Fig. 1—Landmarks (in yellow) digitized on crania of *Leptodactylus bufonius* (Stage 21, FML08011) and semi-landmarks (in green). —**A.** Landmarks in dorsal view (left): 1, most anterior point of the cranium; 2, most anterior point of the nasal; 3, most posterolateral point of the nasal; 4, most medial point of the nasal; 5, premaxilla–maxilla joint; 6, posterior end of the maxilla; 7, most anteromedial point of the frontoparietal; 8, midpoint of the medial margin of the frontoparietal; 9, point of the medial margin of the frontoparietal aligned with the most anterior point of the otic capsule; 10, point of the lateral margin of the frontoparietal aligned with the midpoint of the medial margin of the frontoparietal; 11, caudal end of the skull; 12, most anterior point of the otic capsule; 13, most medial point of the otic capsule; 14, caudal end of the otic capsule; 15, lateral margin of the crista parotica; 16, distal end of the zygomatic ramus of the squamosal; 17, distal end of the otic ramus of the squamosal; 18, distal end of the descendent ramus of the squamosal; 19, anterior end of the quadratojugal; 20, posterior end of the quadratojugal; 21, caudal end of the occipital condyle. —**B.** Landmarks and semi-landmarks in ventral view (left): 1, most anteromedial point of the premaxilla; 2, anterolateral point of the premaxilla; 3, posterolateral point of the premaxilla; 4, posteromedial point of the premaxilla; 5, medial end of the neopalatine; 6, midpoint of the neopalatine (semi-landmark between Landmarks 5 and 7); 7, lateral end of the neopalatine; 8, anterior end of the parasphenoid; 9, midpoint of the lateral margin of the cultriform process of parasphenoid; 10, point of union between the cultriform process of the parasphenoid and the ala of parasphenoid; 11, most anterolateral point of the ala of the parasphenoid; 12, most posterolateral point of the ala of the parasphenoid; 13, posterior end of the parasphenoid; 14, distal end of the anterior ramus of the pterygoid; 15, point of intersection between the anterior and medial rami of the pterygoid; 16, midpoint of the media ramus of pterygoids (semi-landmark between Landmarks 15 and 17); 17, distal end of the medial ramus of the pterygoid; 18, point of intersection between the medial and the posterior rami; 19, distal end of the posterior ramus of the pterygoid; 20, distal end of the anterior ramus of the vomer; 21, distal end of the medial ramus of the vomer; 22, point of intersection point between anterior and posterior rami of the vomer; 23, posterior end of the posterior ramus of the vomer; 24, medial point of the vomer; 25,medial point of the dentigerous process; 26, midpoint of the dentigerous process of the vomer (semi-landmark between Landmarks 25 and 27); 27, most lateral point of the dentigerous process of the vomer.

46). In Stages 0, 1, and 4–13, the bone is mineralized, although ossification occurs in the area next to the frontoparietals. In Stages 2 and 3 and 14–21, the prootics are ossified.

Nasal. The paired bones begin to ossify in Stage 43. In Stages 43, 0, 4 and from 18–21, the nasals resemble those of adults in shape and relative size, being triangular with rounded margins. In specimens in Stages 46 and 2, the nasals are oval. In Stages 1, 3, and 5–8, they have small and triangular nasals, with rounded margins; from Stages 9–17, they have sharp edges. In adult *L. bufonius* the tectum nasi and nasals are synostosed; this is not observed in the postmetamorphic stages.

Tectum nasi and solum nasi. Both elements are cartilaginous in the stages studied. The tectum nasi is not synostosed with the nasal as it is in some adults. The prenasal process is present and cartilaginous in Stages 43, 0, 1, 4, and 9–21, but it is not noticeable in Stages 46, 2, 3, and 5–8.

Frontoparietal. They are posteriorly expanded and rounded, and overlap the prootics, but do not reach the foramen magnum. The frontoparietal fenestra is open anteriorly in Stage 14, and anteriorly and posteriorly in Stages 43, 46, 3, 7, and 15–21. The frontoparietals are ossified in all specimens, except for those from Stages 9–16, which are mineralized.

Parasphenoid. From Stages 43–21, the parasphenoid has a tripartite shape. While the posteromedial process is rectangular, the cultriform process is rectangular or oval, and anteriorly serrated. The cultriform process is ossified in all the specimens, except in Stage 43, when it is mineralized, a condition shared with the alae and the posteromedial process.

Neopalatine. These elements are two cartilaginous, diagonally oriented bars in Stage 43. In Stage 46, they are thin, ossified, and posteriorly concave bars. From Stages 10–21, they are elongated and straight, resembling those of an adult.

Table 2 Ossification sequence of *Leptodactylus bufonius* through metamorphs and postmetamorph stages. Blue cells, cartilaginous; pink cells, mineralized or with partial ossification; red cells, ossified; empty cells, the structure is indistinguishable

		43	43	46	0	1	2	3	4	5	6	7	8	9	10	11	12	13	14	15	16	17	18	19	20	21	Adult (N = 10)
Transverse process																											
Epicoracoid cartilage																											
Omosternum																											
Procoracoid																											
Sternum	Mesosternum																										
	Xiphisternum																										
Clavicle																											
Coracoid																											
Scapula																											
Cleithrum																											
Suprascapula																											
Humerus	Epiphysis																										
	Diaphysis																										
Radioulnae	Epiphysis																										
	Diaphysis																										
Carpal																											
Phalange	Epiphysis																										
	Diaphysis																										
Palmar sesamoid																											
Pararadial sesamoid																											
Glide metacarpals-phalanges																											
Glide between segment phalanges 1 and 2																											
Ilium																											
Sesamoids of the sacral diapophysis																											
Pubis																											
Ischium																											
Femur	Diaphysis																										
	Epiphysis																										
Tibiofibula	Diaphysis																										
	Epiphysis																										
Graciella Sesamoid																											
Cartilage sesamoid																											
Tarsal sesamoid																											

(continued)

Table 2 (continued)

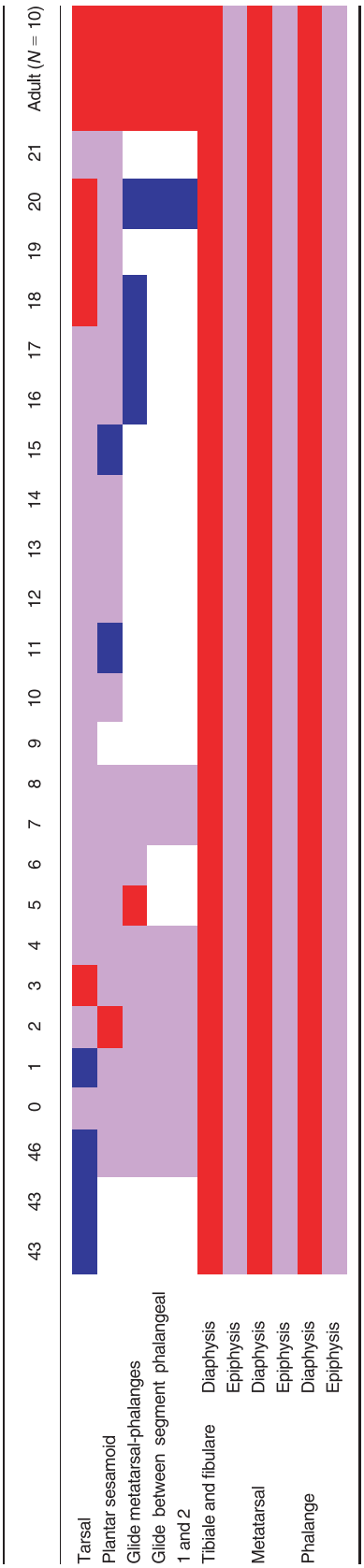

Vomer. Each vomer is composed of four distinct portions—viz., the anterior, the prechoanal, the postchoanal and dentigerous processes. In metamorphic Stage 43, the rami of the vomer are slightly differentiated and the dentigerous process is present. From Stage 5 onwards, the processes are well differentiated. In Stages 46–4, the dentigerous process is absent. The vomers are small, partially developed from Stages 0–17, and ossified from Stages 18–21.

Upper jaw. The premaxillae and maxillae are totally ossified in Stage 43. In the earliest stage studied (Stage 43), the maxillae occupy approximately 40% of the lateral margin and, in postmetamorphic stages, they occupy about 80%.

Lower jaw. The lower jaw consists of Meckel's cartilages plus three pairs of bony elements: mentomeckelian bones, dentaries, and angulosplenials. All these bones are ossified in Stage 43 (Fig. 3).

Squamosal. These bones consist of three rami arranged in a characteristic T-shape: the ventral, otic, and zygomatic rami, all of which are ossified in Stage 43. The zygomatic ramus is straight from Stages 43–4. During Stage 5, the squamosal grows and takes an arcuate (curved anteriorly) shape in the lateral plane. In postmetamorphic stages, the otic ramus reaches and overlaps the border of the crista parotica. The inclination of the squamosal gradually changes from perpendicular (Stage 43) to describe a 45° angle with the horizontal plane of the skull in the adult.

Pterygoid. Although absent in Stage 43, the pterygoids are ossified and typically bear three rami from Stages 46–21. The medial ramus rests on the prootics from Stages 0–21. This arm is straight in Stages 46–4; from Stages 5–21, it is arcuate. The length of the medial ramus relative to the posterior one varies: from Stages 46–2, and in Stages 9, 10, 13, and 14, the medial ramus is approximately equal to the posterior ramus; in the remaining stages, the length of the anterior ramus is shorter than the posterior one. The length of the posterior ramus is less than half of the anterior one from Stages 46–9; it is half the length of the anterior ramus from Stages 10–21.

Quadratojugal. The quadratojugals complete the maxillary arch posteriorly. In Stage 43, the quadratojugals are absent. In Stage 46 and postmetamorphic specimens (from Stages 0–21), the quadratojugal is visible as a thin, ossified stick.

Hyoid apparatus

The apparatus consists of a central corpus, the hyoid plate, which bears four pairs of processes: hyale, anterolateral, posterolateral, and posteromedial. The hyoid plate is present from postmetamorphic Stage 0 onwards. Beginning in this stage, the posteromedial processes ossify and the hyoid plate

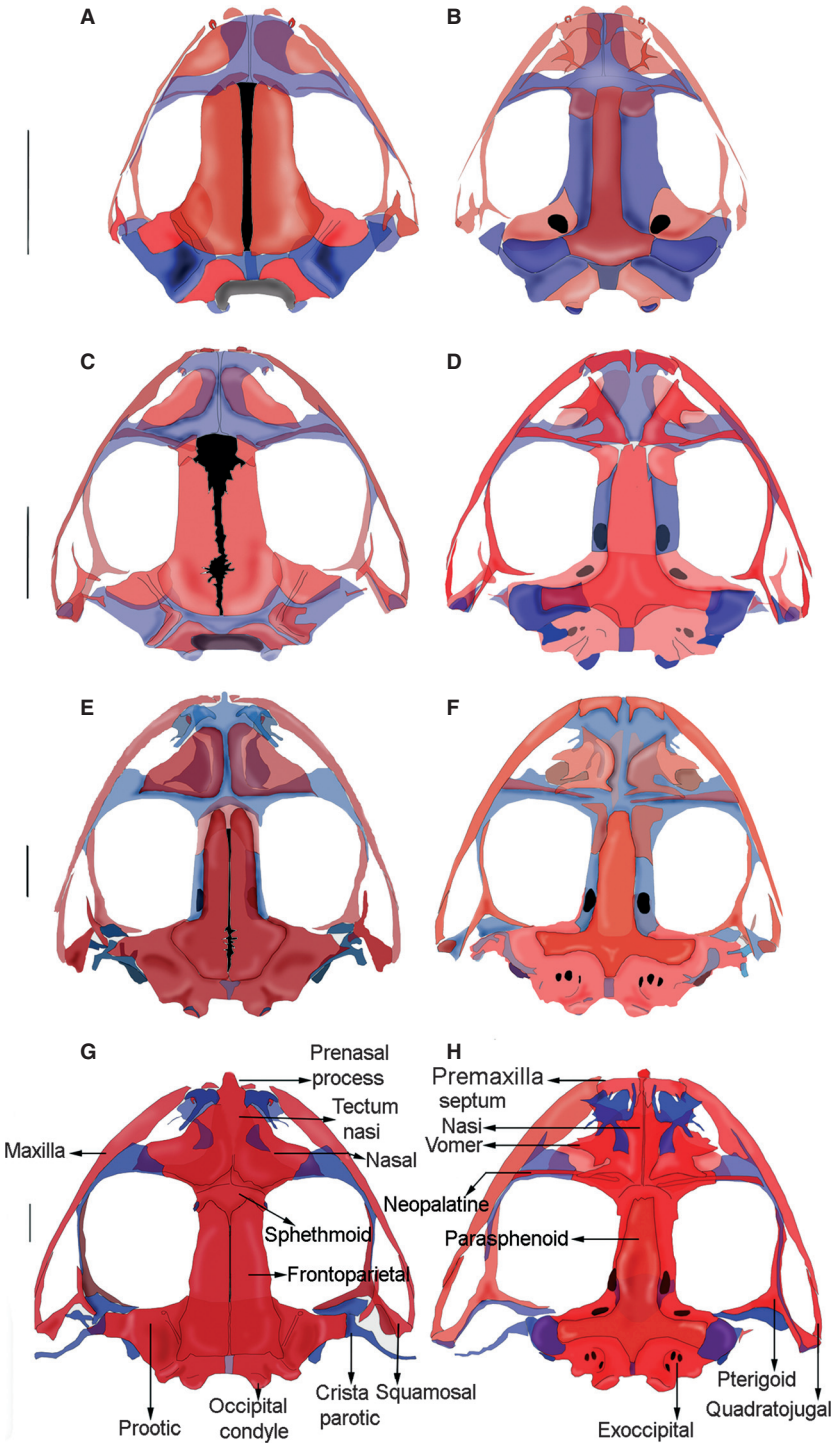

Fig. 2—Dorsal and ventral views of the cranium of *Leptodactylus bufonius*. —**A** and **B.** Dorsal and ventral views of Stage 0 (FML00256-249); —**C** and **D.** Dorsal and ventral views of Stage 8 (FML00256-202); —**E** and **F.** Dorsal and ventral views of Stage 21 (FML08011); —**G** and **H.** Dorsal and ventral views of an adult (FML00672). Blue, red and black denote cartilage, bone and foramina, respectively. Note the gradual closure of the frontoparietal fenestra, the ossification and fusion between prootic and exoccipital, the ossification and synostosis in the nasal region, the pair of centers of ossification corresponding to the sphenethmoid, and the gradual change in the configuration of the neopalatines. Scale line, 2 mm.

mineralizes along the anterior margin of the posteromedial processes (Fig. 3).

Axial Skeleton

The vertebral column is composed of eight procoelous presacral vertebrae, the sacrum, and the urostyle. In Stage 43, the diapophyses of presacral vertebrae I–V are ossified medially. Neither the diapophyses nor the sacral diapophyses are present on presacrals VI–VIII. In the remaining stages (from Stages 46–21), the diapophyses are ossified on all vertebrae. Sesamoids are absent in Stage 43; they are mineralized in Stages 5–8, and cartilaginous in the other stages (Fig. 4).

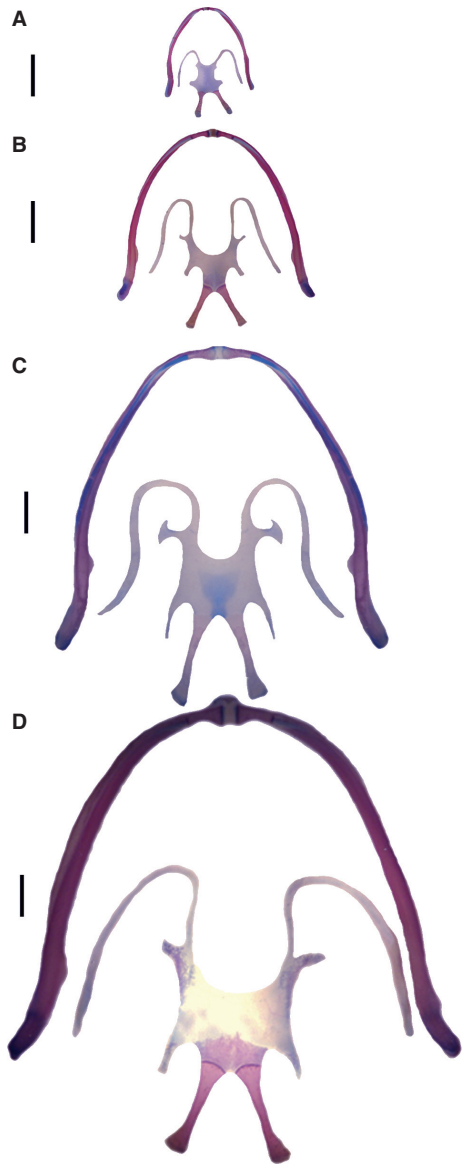

Fig. 3—Lower jaw and hyoid apparatus of *Leptodactylus bufonius*. —**A.** Stage 0; —**B.** Stage 8; —**C.** Stage 21; —**D.** Adult.

Appendicular Skeleton

Pectoral girdle (Fig. 5).

Epicoracoid cartilages. These elements are cartilaginous. In Stage 19, they are mineralized next to the clavicle. In Stage 46, 0 and from Stages 2–6, they are mineralized along the inner side of the bridge. In Stages 7 and 8, they are almost completely mineralized except next to the coracoids (Fig. 5).

Omosternum. It is absent in Stage 43, and cartilaginous in Stages 46, 0–2, 5, and from Stages 9–21. The omosternum is basally mineralized in Stages 3, 4, and 6–8.

Procoracoid. They are cartilaginous in metamorphic stages (43 and 46) and in some postmetamorphic stages (0, 1, 5, 10, and 14). In the remaining stages, the procoracoids are mineralized.

Clavicle. They are ossified from Stage 43 onwards.

Coracoid. They are ossified with cartilaginous distal ends in Stages 43, 46, and 4–8. The distal expanded areas of these elements are mineralized in Stage 1. These bones are already ossified in Stages 2, 3, and from Stage 9 onwards.

Scapulae. These elements show ossification in Stages 43, 46, and 4–8, but remain cartilaginous at the joint between the cleithrum and clavicle. They are already ossified in the other stages.

Cleithrum. The joint between the cleithrum and scapula is cartilaginous in Stages 43 (FML 00587-6), 46, 1, 7, and 8, but mineralized in Stages 2–6. The cleithrum is cartilaginous with the superior ledge mineralized in Stages 9–12, or ossified in Stages 13–21. Only in two of the specimens examined (Stages 43 -FML 00587-5- and 0) is the cleithrum uniformly mineralized.

The suprascapular cartilage, which is continuous with the cleithrum, is mineralized in Stages 7 and 8; it is cartilaginous with mineralized ends in Stages 43(FML 00587-5), 3, 5, and 6.

Sternum. The sternum is a single, long, and flat cartilaginous element that makes up the postzonal pectoral girdle. The element is absent in Stage 43. From Stage 46 onwards, an ossified mesosternum and a cartilaginous xiphisternum are visible. In Stages 1 and 7, the mesosternum is mineralized.

Forelimbs.

Humerus and Radioulna (Fig. 6). Perichondral ossification is complete in the long bones of the forelimbs from Stage 43 onwards. The epiphyses are cartilaginous with mineralization from Stages 43–8, and from Stages 9–21, they are uniformly mineralized. From Stage 43, the humerus has a well-developed crista ventralis (Fig. 6), and the radius and ulna are fused.

Carpals. These short bones are cartilaginous in Stage 43. Secondary centers of ossification are evident in Stage 46. From Stage 18 onwards, the carpals are almost completely ossified (Fig. 6).

Phalanges. The phalangeal formula is 2–2–3–3. The diaphyses are ossified perichondrally from Stage 43 onwards. The epiphyses are mineralized beginning in Stage 43 (Fig. 6). In the 10 adults observed, the epiphyses varied from cartilaginous (two specimens) to mineralized in part (one specimen), and uniformly mineralized (seven specimens).

Palmar sesamoid. This sesamoid is ventral to the carpal bones. The appearance of mineralization and ossification of this element is variable. It is cartilaginous in Stage 43 (FML 00587-6) and from Stages 9–21. In specimen FML 00587-5 (Stage 43), it is absent. The sesamoid is mineralized in Stages 46 and 5–8, and ossified in Stages 0–4. Adults have an ossified

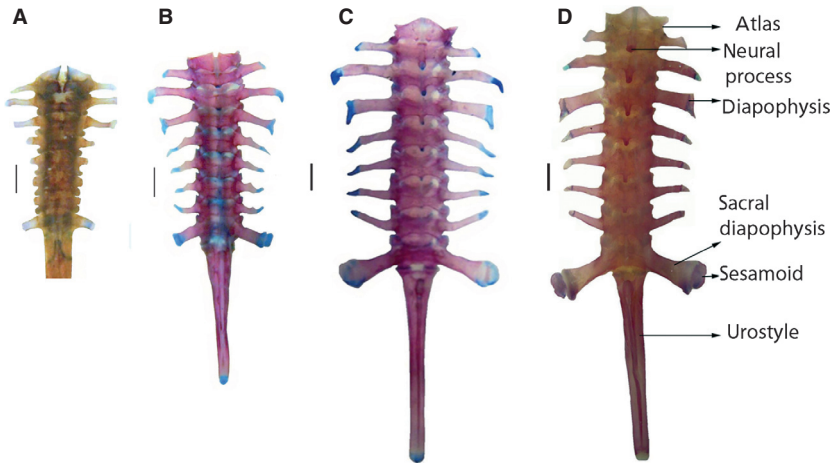

Fig. 4—Vertebral column of *Leptodactylus bufonius*. —**A**. Stage 43 (FML00587-5); —**B.** Stage 14 (FML 12132); —**C**. Stage 21 (FML08011); —**D**. Adult (FML00672). Note the gradual growth of the sacral diapophyses and neural process, and the mineralization of the sesamoid. Scale line, 2 mm.

palmar sesamoid, except for two specimens (FML 09780 and 09779), in which it is cartilaginous.

Pararadial sesamoid. This sesamoid is dorsal to the articulation of the radioulna with the radial; both its occurrence and ossification are variable. In Stage 43, the pararadial appears cartilaginous (FML 00587-6) or mineralized (FML 00587-5). It is cartilaginous in specimens in Stages 9–11, 14, 15, and 21, and mineralized in the specimens observed in Stages 46, 0, 4, 7, 18, and 19. The sesamoid is absent in specimens in Stages 1–3, 5, 6, 12, 13, 16, 17, and 20, and ossified in Stage 8, as well as in all the adults.

Glide sesamoids. These small elements lie ventral to the distal heads of Metacarpalia II–V, and beneath the distal heads of the proximal phalanges of Digits IV and V. The sesamoids of the former group are absent in specimens in Stage 43. They are cartilaginous in specimens in Stages 5, 9–21, and mineralized in specimens in Stages 46, 0–4, and 6–8. They are ossified in adults. The sesamoids of Digits IV and V are absent in Stages 43, 8, 11, and 12; they are cartilaginous in Stages 9, 12–21, and mineralized between Stages 46–7. They are ossified in adults.

Pelvic girdle. The ilium is totally ossified from Stage 43 onwards. The ischium is cartilaginous in Stage 43; partial ossification is visible from Stages 46–8, with the edges of the ischium being cartilaginous and the central area ossified. The element is ossified from Stages 9–21. The pubis is mineralized from Stage 43 onwards (Fig. 7).

Hind limbs and pes.

Femur and tibiofibula. The ossification sequence is the same in both long bones—i.e., the epiphyses are cartilaginous with mineralization from Stages 43–4, and from Stages 5–21, they are uniformly mineralized. Perichondral ossification is complete in the diaphyses from Stage 43 onwards. The epiphyses of adults are mineralized, but three specimens (FML 00672 (A), 09779, 09780) have a cartilaginous articular area (Fig. 8).

Tibiale and fibulare. The epiphyses are cartilaginous with mineralization in Stages 43–4; in the remaining stages, they are uniformly mineralized. Perichondral ossification is complete in the diaphyses from Stage 43 onwards. The tibiale and fibulare are fused in Stage 43 onwards; however, in Stages 43, 1, and 2, the individual epiphyses are evident.

Tarsals. They are cartilaginous in the earlier stages (43, 46, and 1). The appearance of mineralization and ossification is variable. Specimens from Stages 0–21 have mineralized tarsals, except for the specimens in Stages 3, 18–20, in which the tarsals are ossified.

Metatarsals and phalanges. In Stage 43, the epiphyses of these elements are mineralized and the diaphyses are already ossified.

Graciella sesamoid. This small, osseous sesamoid lies ventral to the femur-tibia–fibula joint. It is absent in three specimens in Stages 43 (FML 00587-6), 1, and 2, and mineralized in Stages 46, 3, and 5–8. In the remaining stages, the sesamoid is cartilaginous. The Graciella sesamoid is ossified in adults, but in some specimens (FML 00672(A), 09779, 09780), it retains the areas of cartilage.

Cartilage sesamoid. These sesamoids are present in the tibia and fibula next to the articulation with the tibiafibula. They are mineralized in Stages 46, 0, 2–8, and 17–21. The sesamoid is ossified in only one juvenile (Stage 1) and in most adults; the remaining specimens lack the sesamoid.

Tarsal sesamoid. It is absent in most of the specimens observed but present and mineralized in Stages 19–21.

Plantar sesamoid. This sesamoid is absent in Stages 43 and 9, and is cartilaginous in Stages 11 and 15, and ossified in Stage 2 and in adults. In the remaining stages, the sesamoid is mineralized.

Glide sesamoids. These small elements lie ventral to the distal heads of Metatarsalia II–V, and beneath the distal

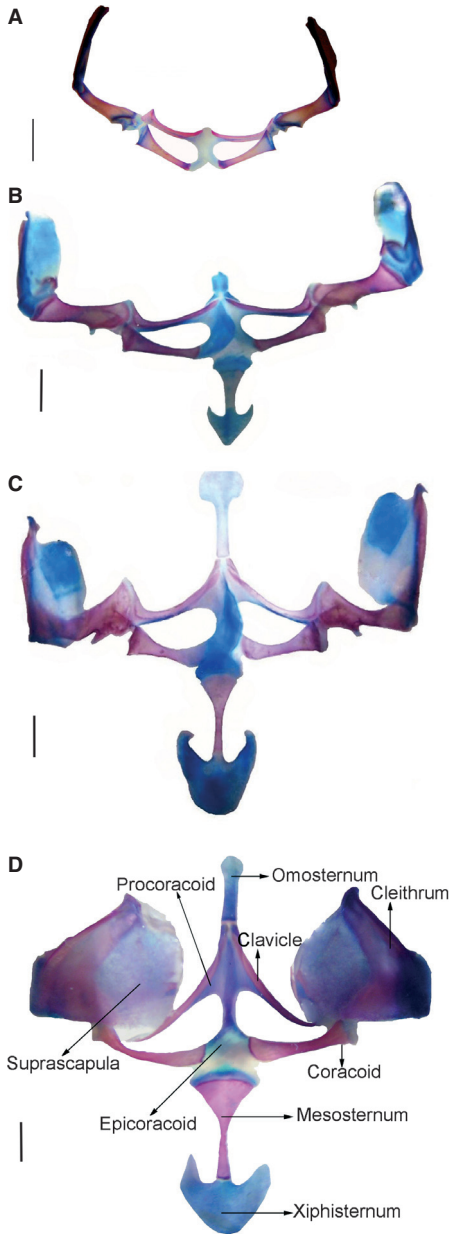

Fig. 5—Pectoral girdle of *Leptodactylus bufonius*. —**A**. Stage 43 (FML00587-5); —**B**. Stage 14 (FML12132); —**C**. Stage 21 (FML08011); —**D**. Adult (FML00672). Note the gradual development and growth of the elements of the sternum. Scale line, 2 mm.

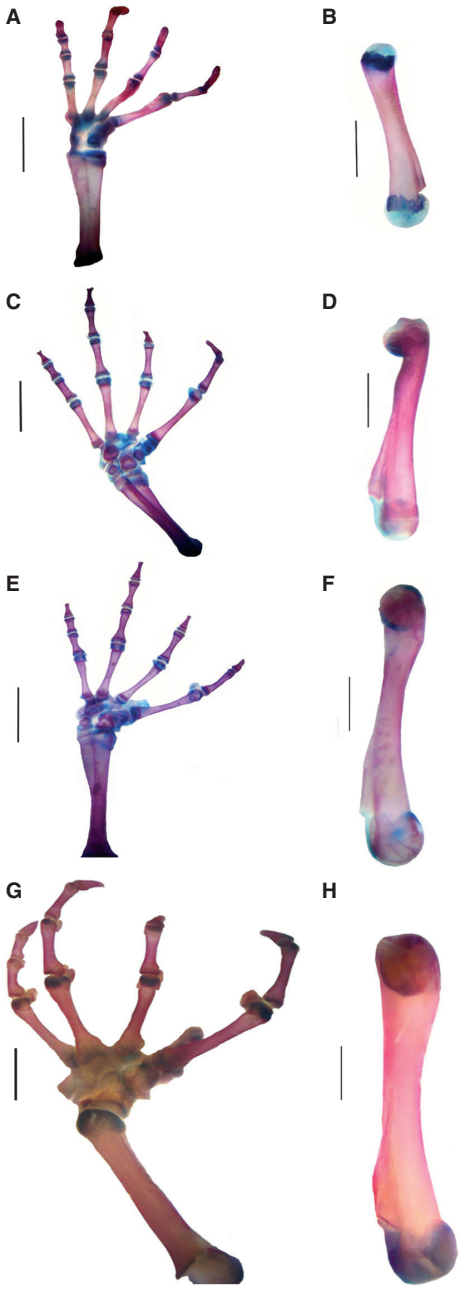

Fig. 6—Humerus and manus of *Leptodactylus bufonius*. —**A, B**. Stage 43 (FML00587-5); —**C, D**. Stage 14 (FML12132); —**E, F**. Stage 21 (FML08011); —**G, H**. Adult (FML00672). Blue and red denote cartilage and bone, respectively. Note the appearance of the center of ossification in the carpals, the gradual mineralization in the epiphyses of the long bones, and the perichondral ossification of the diaphyses. Scale line, 2 mm.

heads of the proximal phalanges of Digits IV and V. The sesamoids of the former group are cartilaginous in Stages 16–18 and 20; mineralized in Stages 46, 0–4, and 6–8; ossified in Stage 5 and adults; and absent in the remaining specimens. The sesamoids of the latter group are absent in most of the specimens. They are cartilaginous in Stage 20, mineralized in Stages 46, 0–4, 7, 8, and ossified in adults.

Changes in skull shape

In the analysis of dorsal skull landmarks, RW1, RW2, and RW3 account for 85.54% of the variation (RW1 = 65.28%,

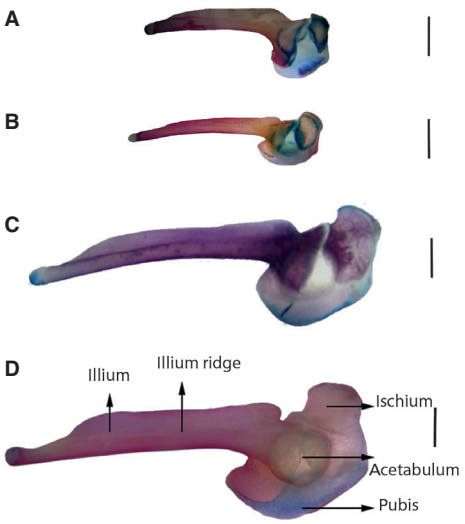

Fig. 7—Pelvic girdle of *Leptodactylus bufonius*. —**A.** Stage 43 (FML00587-5); —**B.** Stage 14 (FML12132); —**C.** Stage 21 (FML08011); —**D.** Adult (FML00672). Note the ilium already ossified in Stage 43; ossification of the ischium is then observed; the pubis remains cartilaginous with mineralization. Scale line: 2 mm.

RW2 = 13.91%, and RW3 = 6.35%; Fig. 9); RW values for dorsal skulls are listed in Table 3. RW1 explains shape changes, involving an extension of the descendent ramus of squamosal (Landmark 18) in a posterolateral direction. The extension of the maxilla is represented by Landmark 6. Both the shape changes imply enlargement of the skull in posterolateral direction. The most anterior point of the nasal (Landmark 2) acquires a more medial position. Finally, shape changes involve the anterior portion of the frontoparietal (Landmark 7). RW2 displays variation involving the otic capsule configuration (Landmarks 12–15); this shape change occurs because the crista parotic (Landmark 15) shifts laterally.

With respect to the skull venter, RW1, RW2, and RW3 account for 81% of the variation (RW1 = 42.75%, RW2 = 23.80%, and RW3 = 14.45%) for the first series (Fig. 10), including the first stages and excluding the landmarks of the dentigerous process of the vomer. Ventral RW values are listed in Table 3. RW1 explains shape changes involving the pterygoid, which change its position from perpendicular to the axial axis to parallel to this axis implying a posterolateral widening of the skull (Landmarks 14, 15, 17, 18, and 19; Semi-landmark 16). The cultriform process

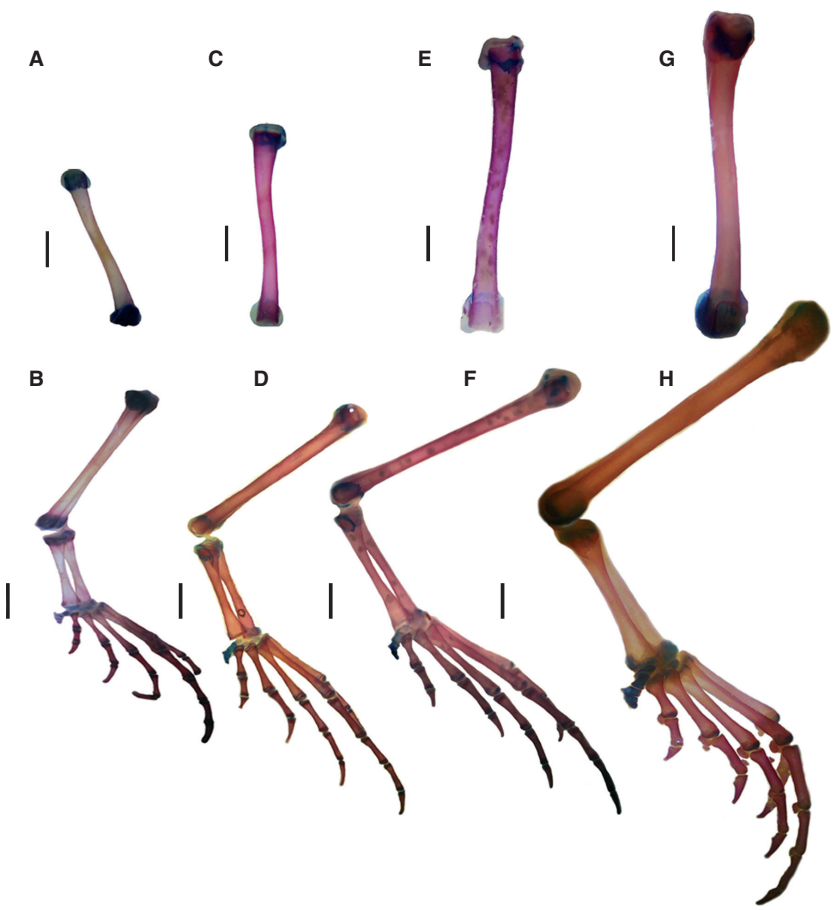

Fig. 8—Hind limbs and pes of *Leptodactylus bufonius*. —**A** and **B.** Stage 43; —**C** and **D.** Stage 14; —**E** and **F.** Stage 21; —**G** and **H**. Adult. Blue and red denote cartilage and bone, respectively. Scale line, 2 mm.

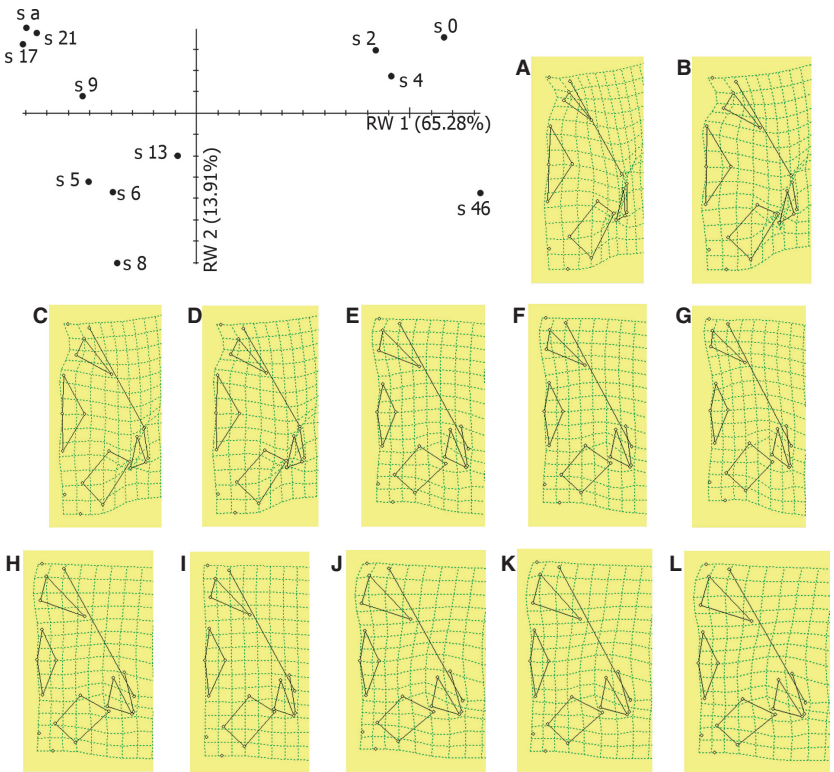

Fig. 9—Scatterplot of the skull in dorsal view on the first two relative warps. The percentage of variance explained by each of the relative warp axis is indicated. Number and letters associated with each point in the scatterplot refer to the stage studied. The thin-plate spline deformation grids illustrate ontogenetic shape changes from Stage 46 to an adult: —**A**. Stage 46 (FML00256-266); —**B**. Stage 0 (FML00256-249); —**C**. Stage 2 (FML00256-246); —**D**. Stage 4 (FML00256-126); —**E**. Stage 5 (FML 00256-235); —**F**. Stage 6 (FML 00256-160); —**G**. Stage 8 (FML00256-202); —**H**. Stage 9 (FML12134); —**I**. Stage 13 (FML12135); —**J**. Stage 17 (FML12133); —**K**. Stage 21 (FML 08011); —**L**. Adult (FML04908).

of the parasphenoid acquires a more rhomboid shape (Landmark 9). The neopalatines elongate and straighten (Landmarks 5 and 7; Semi-landmark 6). The alae of the parasphenoid (Landmarks 11 and 12) extend laterally. In RW2, the shape changes involve the vomer (Landmarks 20–24), in the negative value of the morphospace and posterior ramus of the pterygoid (Landmark 19). In the second series analyzed (excluding the first stages and including the landmarks of the vomer), RW1, RW2, and RW3 account for 89.19% of the variation (RW1 = 57.03%, RW2 = 24.08% and RW3 = 8.08%) (Fig. 11). Ventral RW of this series values are listed in Table 3. RW1 explains shape changes in the dentigerous process of the vomer (Landmarks 25 and 27; Semi-landmark 26), which becomes curve (posteriorly concave). The posterior ramus of the pterygoid elongates in a lateral direction (Landmark 19). Finally, shape changes involve the prolongation of medial side of the vomer (Landmark 24) and neopalatines (Landmark 5). RW2 displays variation involving the medial ramus of the pterygoid (Landmarks15 and 17; Semi-landmark 16).

Discussion

The results show that some elements of the cranium and the postcranium are ossified at metamorphic climax in *Leptodactylus bufonius*. These elements are the following: frontoparietal, the cultriform process of the parasphenoid, prootics, premaxilla, maxilla, squamosal, pterygoid, neopalatines, angulosplenial, dentary, mentomeckelian, mesosternum, and perichondral ossification of the diaphyses of the long bones. However, the mesosternum is only mineralized in two specimens—viz., in juvenile Stages 1 and 7. Other elements remain cartilaginous through the juvenile development stages. Such is the case of the tectum and solum nasi, crista parotica, and xiphisternum. The xiphisternum is scarcely mineralized anteriorly in adults. The tectum and solum nasi, and the crista parotica are completely red-stained in the adult specimens (Ponssa 2008), which clearly shows that these elements go through a late but significant mineralization. In the synostosis observed in the nasal region of the adults, it is evident that the ossification process of the roofing elements continues as the frog matures. Through the postmetamorphic stages, mineralization is observable in the cleithrum, the epiphyses of the long bones, and the pubis.

The striking ossification in *Leptodactylus bufonius* is evident in the presence of strong mineralization in both areas that are usually cartilaginous in anurans (e.g., the nasal region and the epiphyses). This ossification is not as extensive as the hyperossification described in large species, such as *Cerathophrys cornuta* (Wild 1997) and *Pyxicephalus adspersus* (Sheil 1999), or in miniaturized species, such as those of the genus *Brachycephalus* (Hanken 1993; Clemente-Carvalho *et al.* 2009); however, it can be equivalent to the additional mineralization of the tectum nasi and fusion with the nasal described for *Acris blanchardi* (Maglia *et al.* 2007). The degree of ossification

Table 3 Singular values and percent explained for relative warps of dorsal and ventral skull analyses

Relative warp	Singular value	Percent explained (%)	Cum (%)
Dorsal skull			
1	0.27090	65.28%	65.28%
2	0.12505	13.91%	79.19%
3	0.08449	6.35%	85.54%
4	0.07293	4.73%	90.27%
5	0.06381	3.62%	93.89%
6	0.05170	2.38%	96.27%
7	0.03998	1.42%	97.69%
8	0.03275	0.95%	98.65%
9	0.02746	0.67%	99.32%
10	0.02124	0.40%	99.72%
11	0.01776	0.28%	100.00%
Ventral skull (series 1)			
1	0.18840	42.75%	42.75%
2	0.14059	23.80%	66.55%
3	0.10953	14.45%	81.00%
4	0.08816	9.36%	90.36%
5	0.04904	2.90%	93.26%
6	0.04033	1.96%	95.22%
7	0.03773	1.71%	96.93%
8	0.03343	1.35%	98.27%
9	0.02434	0.71%	98.99%
10	0.02368	0.68%	99.66%
11	0.01671	0.34%	100.00%
Ventral skull (series 2)			
1	0.14277	57.03%	57.03%
2	0.09277	24.08%	81.11%
3	0.05373	8.08%	89.19%
4	0.03930	4.32%	93.51%
5	0.03457	3.34%	96.86%
6	0.02585	1.87%	98.73%
7	0.02133	1.27%	100.00%

and/or mineralization is not necessarily correlated with large body size of the frog; in the miniaturized *Acris crepitans*, heavy mineralization would compensate for the poor degree of ossification of most of the bones (Maglia *et al.* 2007). The heavy ossification in *L. bufonius* is hard to relate to both a large size and the mechanism of compensation of the miniaturized frogs; *L. bufonius* is a medium-sized species (male SVL, 51.6 ± 2.0; female SVL, 53.6 ± 2.3 mm; Heyer 1978) relative to other species of the genus. In the *L. fuscus* Group, the reinforcement of the skull, particularly in the nasal region, has been associated with the digging behavior involved in the building of the incubation chamber (Heyer 1978; Ponssa 2008; Ponssa *et al.* 2010b, 2011).

Some skeletal elements are variable in pattern, which makes it difficult to establish an ossification timeline. The observed variability may be biased by the clearing-and-staining technique used, and the time and/or technique of preservation. In these preliminary results, some elements of the pectoral girdle (e.g., epicoracoid cartilage, omosternum, procoracoid, coracoid, scapula, and suprascapula), carpals, tarsals, and sesamoids, show some degree of ossification in earlier stages; however, they are cartilaginous in older individuals. This variance suggests that, in addition to the intrinsic factor that determines the timing of development, extrinsic factors may elicit the osteogenesis. Actually, the movement of the joints during development would be an epigenetic factor to produce the genesis and ossifications of some sesamoids (Le Minor 1987; Giori *et al.* 1993; Benjamin and Ralphs 1998; Carter *et al.* 1998; Sarin *et al.* 1999; Vickaryous and Olson 2007; Kim *et al.* 2009; Abdala and Ponssa 2012). It is in the juvenile stages of development that the frog begins to use the girdles and limbs for saltation. The osteogenesis of the remaining elements follows a gradual sequence of ossification through the postmetamorphic period of development. The exoccipital and the ischium are the first to complete ossification; the nasal and vomer commence ossification in Stage 43, and they complete it in the last juvenile stage studied. The only elements that are not present in metamorphic Stage 43 are the pterygoid, omosternum, sternum, some sesamoids, and the quadratojugal, which are present at the moment of the metamorphic climax (Stage 46).

Skeletal development and sequence of ossification in anurans have been reported in several studies dealing with larval and metamorphic stages (e.g., Bernasconi 1951; Hanken and Hall 1984; Trueb 1985; de Sá 1988; Wiens 1989; de Sá and Trueb 1991; Trueb and Hanken 1992; Púgener and Maglia 1997; Wild 1997, 1999; Maglia and Púgener 1998; Haas 1999; Perotti 2001; Sheil and Alamillo 2005; Banburi and Maglia 2006; Havens 2010). We observed some similarities, as well as differences, in the commencement of ossification of skeletal elements in *Leptodactylus bufonius* and other species of anurans (Table 4). Given the gross anatomical variation in frogs, it may be possible that the timing of skeletogenesis may be related to species-specific differences in the timing of functional capacities during development. Further studies are necessary to elucidate this issue.

Ponssa and Vera Candioti (2012) observed that the metamorphic specimens (Stage 46) of *Leptodactylus* are more variable in skull shape than the adults. Ciampaglio (2002) stated that this kind of shape disparity may be a consequence of ecological or genetic constraints. In *L. bufonius*, the posterolateral area of the skull undergoes the greatest change in shape, becoming conspicuously larger, thereby implying a shape change in the otic region, and growth and rotation to a horizontal position of the squamosals and pterygoids. The shape change described would affect feeding, with the squamosal and pterygoids serving as points of attachment for muscles involved in the jaw closing (Duellman and Trueb 1986). Larson (2005) found shape change and differential scaling in the region of the jaw closure through larval development. The shape change in juvenile development may be associated with either the biomechanical importance of this region as a muscle insertion site or the force of muscle contraction (Larson 2005). Another

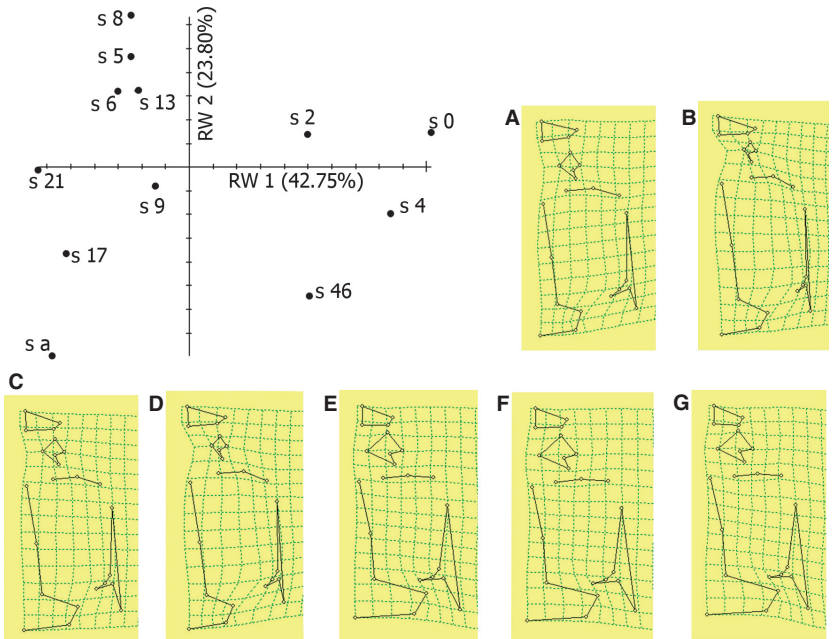

Fig. 10—Scatterplot of the skull in ventral view on the first two relative warps of the first series analyzed. The percentage of variance explained by each of the relative warp axes is indicated. Number and letters associated with each point in the scatterplot refer to the stage studied. The thin-plate spline deformation grids illustrate ontogenic shape changes from Stage 46 to an adult: —**A.** Stage 46 (FML00256-266); —**B**. Stage 0 (FML00256-249); —**C.** Stage 2 (FML00256-246); —**D**. Stage 4 (FML00256-126); —**E**. Stage 5 (FML 00256-235); —**F**. Stage 6 (FML 00256-160); —**G**. Stage 8 (FML00256-202); —**H**. Stage 9 (FML12134); —**I**. Stage 13 (FML12135); —**J**. Stage 17 (FML12133); —**K**. Stage 21 (FML 08011); —**L**. Adult (FML04908).

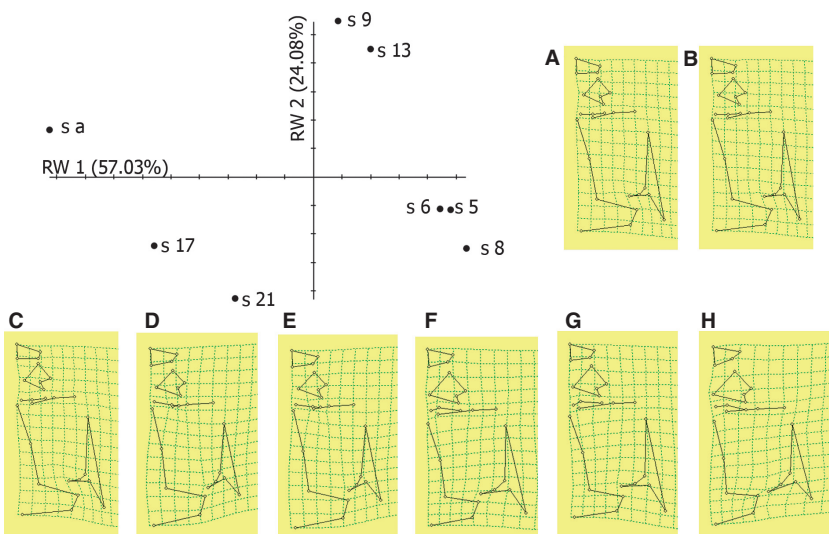

Fig. 11—Scatterplot of the skull in ventral view on the first two relative warps of the second series analyzed. The percentage of variance explained by each of the relative warp axes is indicated. Number and letters associated with each point in the scatterplot refer to the stage studied. The thin-plate spline deformation grids illustrate ontogenic shape changes from Stage 5 to an adult: —**A**. Stage 5 (FML00256-235); —**B**. Stage 6 (FML00256-160); —**C**. Stage 8 (FML00256-202); —**D**. Stage 9 (FML12134); —**E**. Stage 13(FML12135); —**F**. Stage 17 (FML12133); —**G.** Stage 21 (FML08011); —**H**. Adult (FML04908).

morphological modulus of functional importance involves the otic capsules. The shape change and ossification associated with the otic capsules include prootics, exoccipital, and stapes (Cannatella 1999). Adult anurans have greater auditory sensitivity than do larvae (Shofner 1983); hence, this hearing capacity may have been acquired in synchrony with the morphological changes occurring through juvenile development.

Table 4 Comparison between the beginning of the ossification of skeletal elements in *Leptodactylus bufonius* and other species previously studied

	Leptodactylus bufonius	Other species
Exoccipital	Stage 0 (juvenile)	*Leptodactylus chaquensis*: Stage 33 (Perotti 2001). *Ceratophrys cornuta*: Stage 38 (Wild 1997). *Chacophrys pierotti*: Stage 38 (Wild 1999). *Xenopus laevis*: Stage 35–38 (Trueb and Hanken 1992, Bernasconi 1951). *Spea multiplicata:* Stage 38 (Banburi and Maglia 2006). *Pyxicephalus adspersus*: Stage 33 (Hass 1999). *Phyllomedusa vaillanti*: Stage 38 (Sheil and Alamillo 2005). *Acris blanchardi*: Stage 36 (Havens 2010)
Frontoparietal	Stage 43	*Leptodactylus chaquensis*: Stage 38 (Perotti 2001). *Ceratophrys cornuta*: Stage 38 (Wild 1997). *Chacophrys pierotti*: Stage 38 (Wild 1999). *Xenopus laevis*: Stage 34 and 35 (Trueb and Hanken 1992, Bernasconi 1951). *Phyllomedusa vaillanti*: Stage 41 (Sheil and Alamillo 2005). *Spea multiplicata:* Stage 37 (Banburi and Maglia 2006). *Pyxicephalus adspersus*: Stage 34 (Hass 1999). *Acris blanchardi*: Stage 36 (Havens 2010)
Prootic	Stage 43	*Leptodactylus chaquensis*: Stage 39 (Perotti 2001) *Ceratophrys cornuta*: Stage 38 (Wild 1997). *Chacophrys pierotti*: Stage 42 (Wild 1999). *Xenopus laevis*: Stage 35–39 (Trueb and Hanken 1992). *Spea multiplicata*: Stage 41 (Banburi and Maglia 2006). *Pyxicephalus adspersus*: Stage 40 (Hass 1999). *Phyllomedusa vaillanti*: Stage 38 (Sheil and Alamillo 2005). *Acris blanchardi*: Stage 36 (Havens 2010)
Maxilla	Stage 43	*Leptodactylus chaquensis*: Stage 42(Perotti 2001) *Ceratophrys cornuta*: Stage 42 (Wild 1997). *Chacophrys pierotti*: Stage 42 (Wild 1999). *Xenopus laevis*: Stage 39 (Trueb and Hanken 1992). *Spea multiplicata*: Stage 41 (Banburi and Maglia 2006). *Pyxicephalus adspersus*: Stage 41 (Hass 1999). *Phyllomedusa vaillanti*: Stage 42 (Sheil and Alamillo 2005). *Acris blanchardi*: Stage 41 (Havens 2010)
Premaxilla	Stage 43	*Leptodactylus chaquensis*: Stage 40 (Perotti 2001). *Ceratophrys cornuta*: Stage 42 (Wild 1997). *Chacophrys pierotti*: Stage 42 (Wild 1999). *Xenopus laevis*: Stage 40 (Trueb and Hanken 1992). *Spea multiplicata*: Stage 39 (Banburi and Maglia 2006). *Pyxicephalus adspersus*: Stage 39 (Hass 1999). *Phyllomedusa vaillanti*: Stage 42 (Sheil and Alamillo 2005). *Acris blanchardi*: Stage 40 (Havens 2010)
Parasphenoid	Stage 43	*Leptodactylus chaquensis*: Stage 34 (Perotti 2001) *Pyxicephalus adspersus*: Stage 33 (Hass 1999). *Xenopus laevis*: Stage 35 (Trueb and Hanken 1992, Bernasconi 1951). *Ceratophrys cornuta*: Stage 38 (Wild 1997). *Chacophrys pierotti*: Stage 38 (Wild 1999). *Spea multiplicata:* Stage 35 (Banburi and Maglia 2006) *Phyllomedusa vaillanti*: Stage 38 (Sheil and Alamillo 2005). *Acris blanchardi*: Stage 32 (Havens 2010).
Squamosal	Stage 43	*Leptodactylus chaquensis*: Stage 42 (Perotti 2001). *Ceratophrys cornuta*: Stage 43 (Wild 1997). *Chacophrys pierotti*: Stage 43 (Wild 1999). *Xenopus laevis*: Stage 43–44 (Trueb and Hanken 1992). *Spea multiplicata:* Stage 44 (Banburi and Maglia 2006). *Pyxicephalus adspersus*: Stage 40 (Hass 1999). *Phyllomedusa vaillanti*: Stage 45 (Sheil and Alamillo 2005). *Acris blanchardi*: Stage 46 (Havens 2010)
Dentary	Stage 43	*Leptodactylus chaquensis*: Stage 43 (Perotti 2001). *Ceratophrys cornuta*: Stage 44 (Wild 1997). *Chacophrys pierotti*: Stage 43 (Wild 1999). *Xenopus laevis*: Stage 41–42 (Trueb and Hanken 1992). *Spea multiplicata*: Stage 44 (Banburi and Maglia 2006). *Pyxicephalus adspersus*: Stage 43 (Hass 1999). *Phyllomedusa vaillanti*: Stage 45 (Sheil and Alamillo, 2005). *Acris blanchardi*: Stage 45 (Havens 2010).
Angulosplenial	Stage 43	*Leptodactylus chaquensis*: Stage 42 (Perotti 2001). *Ceratophrys cornuta*: Stage 44 (Wild 1997). *Chacophrys pierotti*: Stage 43 (Wild 1999). *Xenopus laevis*: Stage 41 (Trueb and Hanken 1992). *Spea multiplicata*: Stage 44 (Banburi and Maglia 2006). *Pyxicephalus adspersus*: Stage 41 (Hass 1999). *Phyllomedusa vaillanti*: Stage 45 (Sheil and Alamillo 2005). *Acris blanchardi*: Stage 45 (Havens 2010).
Vomer	Stage 43	*Leptodactylus chaquensis*: Stage 43 (Perotti, 2001). *Ceratophrys cornuta*: Stage 44 (Wild 1997). *Chacophrys pierotti*: Stage 45 (Wild 1999). *Xenopus laevis*: Stage 43–44 (Trueb and Hanken, 1992). *Spea multiplicata*: Stage 44 (Banburi and Maglia 2006). *Pyxicephalus adspersus*: Stage 43 (Hass 1999). *Phyllomedusa vaillanti*: Stage 45 (Sheil and Alamillo 2005). *Acris blanchardi*: Stage 44 (Havens 2010)
Neopalatine	Stage 43	*Leptodactylus chaquensis*: postmetamorphic stages (Perotti 2001). *Pyxicephalus adspersus*: Stage 44 (Hass 1999)
Pterygoid	Stage 46	*Leptodactylus chaquensis*: Stage 44 (Perotti 2001). *Ceratophrys cornuta*: Stage 44 (Wild 1997). *Chacophrys pierotti*: Stage 43 (Wild 1999). *Xenopus laevis*: Stage 42 (Trueb and Hanken 1992). *Spea multiplicata*: Stage 45 (Banburi and Maglia 2006). *Pyxicephalus adspersus*: Stage 44 (Haas 1999). *Acris blanchardi*: Stage 46 (Havens 2010).
Quadratojugal	Stage 46	*Leptodactylus chaquensis*: Stage 45 (Perotti 2001) *Ceratophrys cornuta*: Stage 44 (Wild 1997). *Chacophrys pierotti*: Stage 43 (Wild 1999). *Pyxicephalus adspersus*: Stage 44 (Haas 1999). *Acris blanchardi*: Stage 46 (Haven 2010).
Nasal	Stage 43	*Leptodactylus chaquensis*: Stage 42 (Perotti 2001) *Ceratophrys cornuta*: Stage 44 (Wild 1997). *Chacophrys pierotti*: Stage 45 (Wild 1999). *Xenopus laevis*: Stage 40–41 (Trueb and Hanken 1992) *Pyxicephalus adspersus*: Stage 42 (Hass 1999). *Spea multiplicata*: Stage 39 (Banburi and Maglia 2006). *Acris blanchardi*: Stage 42 (Havens 2010)
Mentomeckelian	Stage 43	*Leptodactylus chaquensis*: Stage 45 (Perotti 2001). *Spea multiplicata:* mid-age juvenil (Banburi and Maglia 2006). *Pyxicephalus adspersus*: Stage 44 (Haas 1999). *Acris blanchardi*: Stage 46 (Havens 2010).
Sphenethmoid	Stage 0 (juvenile)	*Leptodactylus chaquensis*: postmetamorphic stage (Perotti 2001). *Xenopus laevis*: Stage 44 (Trueb and Hanken 1992) *Spea multiplicata*: Stage 46 (Banburi and Maglia 2006). *Acris blanchardi*: after Stage 46 (Havens 2010).
Transverse processes	Stage 43	*Xenopus laevis*: Stage 44 (Trueb and Hanken 1992, Smit 1953).

Table 4 (continued)

	Leptodactylus bufonius	Other species
Coracoid	Stage 43	*Leptodactylus chaquensis*: Stage 39 (Perotti 2001). *Ceratophrys cornuta*: Stage 38 (Wild 1997). *Chacophrys pierotti*: Stage 42 (Wild, 1999). *Spea multiplicata:* Stage 39 (Banburi and Maglia 2006). *Pyxicephalus adspersus*: Stage 38 (Hass 1999). *Phyllomedusa vaillanti*: Stage 38 (Sheil and Alamillo 2005). *Acris blanchardi*: Stage 38 (Havens 2010). *Xenopus laevis*: Stage 39–41 (Trueb and Hanken, 1992)
Clavicle	Stage 43	*Leptodactylus chaquensis*: Stage 38 (Perotti 2001). *Ceratophrys cornuta*: Stage 38 (Wild 1997). *Chacophrys pierotti*: Stage 38 (Wild 1999). *Spea multiplicata*: Stage 37 (Banburi and Maglia 2006). *Pyxicephalus adspersus*: Stage 38 (Hass 1999). *Phyllomedusa vaillanti*: Stage 38 (Sheil and Alamillo 2005). *Acris blanchardi*: Stage 38 (Haven 2010). *Xenopus laevis*: Stage 39–41 (Trueb and Hanken 1992)
Procoracoids	Stage 2	*Leptodactylus chaquensis*: postmetamorphic stage (Perotti 2001)
Scapula	Stage 43	*Leptodactylus chaquensis*: Stage 39 (Perotti 2001). *Ceratophrys cornuta*: Stage 38 (Wild 1997). *Chacophrys pierotti*: Stage 38 (Wild 1999). *Spea multiplicata*: Stage 38 (Banburi and Maglia 2006). *Pyxicephalus adspersus*: Stage 35 (Hass 1999). *Phyllomedusa vaillanti*: Stage 38 (Sheil and Alamillo 2005). *Acris blanchardi*: Stage 37 (Haven 2010). *Xenopus laevis*: Stage 41–42 (Trueb and Hanken 1992)
Humerus	Stage 43	*Leptodactylus chaquensis*: Stage 36 (Perotti 2001). *Ceratophrys cornuta*: Stage 38 (Wild 1997). *Chacophrys pierotti*: Stage 38 (Wild 1999). *Spea multiplicata:* Stage 37 (Banburi and Maglia 2006). *Pyxicephalus adspersus*: Stage 35 (Hass 1999). *Phyllomedusa vaillanti*: Stage 38 (Sheil and Alamillo 2005). *Acris blanchardi*: Stage 37 (Haven 2010). *Xenopus laevis*: Stage 39 (Trueb and Hanken 1992, Bernasconi 1951, Brown 1980)
Radioulna	Stage 43	*Leptodactylus chaquensis*: Stage 38 (Perotti 2001). *Ceratophrys cornuta*: Stage 38 (Wild 1997). *Chacophrys pierotti*: Stage 38 (Wild 1999). *Spea multiplicata:* Stage 37 (Banburi and Maglia 2006). *Pyxicephalus adspersus*: Stage 35 (Hass 1999). *Phyllomedusa vaillanti*: Stage 38 (Sheil and Alamillo 2005). *Acris blanchardi*: Stage 37 (Haven 2010). *Xenopus laevis*: Stage 39 (Trueb and Hanken 1992, Bernasconi 1951, Brown 1980)
Metacarpals	Stage 43	*Spea multiplicata*: Stage 39 (Banburi and Maglia 2006). *Pyxicephalus adspersus*: Stage 38 (Hass 1999). *Phyllomedusa vaillanti*: Stage 38 (Sheil and Alamillo 2005). *Acris blanchardi*: Stage 38 (Haven 2010). *Xenopus laevis*: Stage 39 (Brown 1980)
Hand Phalanges	Stage 43	*Leptodactylus chaquensis*: Stage 39 (Perotti 2001). *Ceratophrys cornuta*: Stage 38 (Wild 1997). *Chacophrys pierotti*: Stage 42 (Wild 1999). *Spea multiplicata:* Stage 39–40 (Banburi and Maglia 2006). *Pyxicephalus adspersus*: Stage 38 (Hass 1999). *Phyllomedusa vaillanti*: Stage 38 (Sheil and Alamillo 2005). *Acris blanchardi*: Stage 38 (Haven 2010). *Xenopus laevis*: Stage 41–43 (Trueb and Hanken 1992)
Ischium	Stage 46	*Ceratophrys cornuta*: Stage 44 (Wild 1997). *Acris blanchardi* and *Pseudacris crucifer*: Stage 40 (Havens 2010). *Xenopus laevis*: Stage 41 (Bernasconi 1951, Nieuwkoop and Faber 1956, Trueb and Hanken 1992). *Spea multiplicata:* Stage 43 (Banburi and Maglia 2006). *Pyxicephalus adspersus*: Stage 41 (Hass 1999). *Phyllomedusa vaillanti*: Stage 42 (Sheil and Alamillo 2005)
Illium	Stage 43	*Leptodactylus chaquensis*: Stage 35 (Perotti 2001). *Ceratophrys cornuta*: Stage 35 (Wild 1997). *Chacophrys pierotti*: Stage 38 (Wild 1999). *Xenopus laevis*: Stage 41(Bernasconi 1951, Nieuwkoop and Faber 1956, Trueb and Hanken 1992). *Spea multiplicata:* Stage 36 (Banburi and Maglia 2006). *Pyxicephalus adspersus*: Stage 36 (Hass 1999). *Phyllomedusa vaillanti*: Stage 38 (Sheil and Alamillo 2005). *Acris blanchardi*: Stage 38 (Haven 2010). *Xenopus laevis*: Stage 39 (Trueb and Hanken 1992, Bernasconi 1951, Brown 1980)
Pubis	Stage 43	*Xenopus laevis*: Stage 41 (Bernasconi 1951, Nieuwkoop and Faber 1956, Trueb and Hanken 1992). *Phyllomedusa vaillanti*: Stage 42 (Sheil and Alamillo 2005)
Femur	Stage 43	*Leptodactylus chaquensis*: Stage 37 (Perotti 2001). *Ceratophrys cornuta*: Stage 35 (Wild 1997). *Chacophrys pierotti*: Stage 38 (Wild 1999). *Spea multiplicata:* Stage 36 (Banburi and Maglia 2006). *Pyxicephalus adspersus*: Stage 34 (Hass 1999). *Phyllomedusa vaillanti*: Stage 38 (Sheil and Alamillo 2005). *Acris blanchardi*: Stage 36 (Haven 2010). *Xenopus laevis*: Stage 39 (Trueb and Hanken 1992, Bernasconi 1951, Brown 1980)
Tibiofibula	Stage 43	*Leptodactylus chaquensis*: stage 37 (Perotti 2001). *Ceratophrys cornuta*: Stage 35 (Wild 1997). *Chacophrys pierotti*: Stage 38 (Wild 1999). *Spea multiplicata:* Stage 37 (Banburi and Maglia 2006). *Pyxicephalus adspersus*: Stage 34 (Hass 1999). *Phyllomedusa vaillanti*: Stage 38 (Sheil and Alamillo 2005). *Acris blanchardi*: Stage 37 (Haven 2010). *Xenopus laevis*: Stage 39 (Trueb and Hanken 1992, Bernasconi 1951, Brown 1980)
Tibiale fibulare	Stage 43	*Leptodactylus chaquensis*: Stage 37 (Perotti 2001). *Ceratophrys cornuta*: Stage 38 (Wild 1997). *Chacophrys pierotti*: Stage 42 (Wild 1999). *Spea multiplicata*: Stage 38 (Banburi and Maglia 2006). *Pyxicephalus adspersus*: Stage 34 (Hass 1999). *Phyllomedusa vaillanti*: Stage 38 (Sheil and Alamillo 2005). *Acris blanchardi*: Stage 37 (Haven 2010). *Xenopus laevis*: Stage 39 (Trueb and Hanken 1992, Bernasconi 1951)
Metatarsals	Stage 43	*Spea multiplicata:* Stage 37 (Banburi and Maglia 2006). *Pyxicephalus adspersus*: Stage 35–38 (Hass 1999). *Phyllomedusa vaillanti*: Stage 38 (Sheil and Alamillo 2005). *Acris blanchardi*: Stage 37 (Haven 2010). *Xenopus laevis*: Stage 39 (Trueb and Hanken 1992)
Foot phalanges	Stage 43	*Leptodactylus chaquensis*: Stage 38 (Perotti 2001). *Ceratophrys cornuta*: Stage 38 (Wild 1997). *Chacophrys pierotti*: Stage 42 (Wild 1999). *Spea multiplicata:* Stage 37, 39 and 40 (Banburi and Maglia 2006). *Pyxicephalus adspersus*: Stage 38 (Hass 1999). *Phyllomedusa vaillanti*: Stage 38 (Sheil and Alamillo 2005). *Acris blanchardi*: Stage 37 (Haven 2010)

Anatomically, postmetamorphic developmental changes in these anurans involves increase in size, skeletal maturity, and change in shape. In anurans, the greatest variation in the extent of ossification and morphology takes place in larvae. During postmetamorphic development, most cranial bones complete their changes in shape (Djorović and Kalezić 2000). The morphogenetic process occurring throughout the postmetamorphic stages is noticeable (Trueb and Hanken 1992). Because frogs are subject to intense selection through predation (Arnold and Wassersug 1978), it has been proposed that the period from a swimming larva to a hopper frog is critical for the survival of anurans. Experimentally, it has been demonstrated that metamorphs do not swim as efficiently as earlier-stage tadpoles that lack forelimbs; however, these, in contrast to postmetamorphic–stage frogs, are ineffective hoppers. Thus, locomotive performance of tadpoles is poor during their metamorphosis (Wassersug and Sperry 1997). Our data demonstrate that many skeletal elements, such as those of the locomotor system, have not yet completed their development at metamorphic climax. Thus, we assume that juveniles do not move as efficiently as do adults and that they probably are more vulnerable to predation. The dramatic morphological changes that characterize the juvenile period probably are correlated with ecology and function. There is a synchrony between the morphological maturity of key systems, such as locomotion and sensation, and their functionality in juveniles stage in preparation functionality in adults. The significant changes in shape and tissue differentiation that occur during the transition from the juvenile to the adult deserve further consideration.

Acknowledgements

We thank Luisa Montivero for her help with English, and Gonzalo Gallego Heras for his help with specimen preparation**.** The research was funded by CONICET (Grant number: PIP 112-200801-00225), FONCYT (Grant number: PICT 2008-0578), and CIUNT (Grant number: G430).

References

Abdala, V. and Ponssa, M. L. 2012. Life in the slow lane: the effect of reduced mobility on tadpole limb development. – *The Anatomical Record* **295**: 5–17.

Arnold, S. J. and Wassersug, R. J. 1978. Differential predation on metamorphic -anurans by garter snakes *(Thamnophis):* social behaviour as a possible defense. – *Ecology* **59**: 1014–1022.

Banburi, B. and Maglia, A. M. 2006. Skeletal Development of the Mexican Spadefoot, *Spea multiplicata*(Anura: Pelobatidae). – *Journal of Morphology* **267**: 803–821.

Benjamin, M. and Ralphs, J. R. 1998. Fibrocartilage in Tendons and Ligaments: An Adaptation to Compressive Load. – *Journal of Anatomy* **193**: 481–494.

Bernasconi, A. F. 1951. Uber den Ossifikationsmodusbei *Xenopus laevis* (Daudain). – *Memoirs of the Society Helvetic of Natural Sciences* **79**: 191–252.

Bookstein, F. L. 1991. Morphometric Tools for Landmark Data. Geometry and Biology. Cambridge University Press, New York.

Brown, S. M. 1980. *Comparative Ossification in Tadpoles of the Genus* Xenopus *(Anura, Pipidae)*. Master's thesis, San Diego State Univeristy, San Diego.

Cannatella, D. 1999. Architecture: cranial and axial musculoskeleton. In: McDiarmid, R. W. and Altig, R. (Eds): Tadpoles. The Biology of Anuran Larvae, pp. 52–91. The University of Chicago Press, Chicago.

Cardini, A. 2003. The geometry of the marmot (Rodentia; Sciuridae) mandible: phylogeny and patterns of morphological evolution. – *Systematic Biology* **52**: 186–205.

Cardini, A. and O'Higgins, P. O. 2005. Post-natal ontogeny of the mandible and ventral cranium in *Marmota* (Rodentia, Sciuridae): allometry and phylogeny. – *Zoomorphology* **124**: 189–203.

Carter, D. R., Mikic, B. and Padian, K. 1998. Epigenetic mechanical factors in the evolution of long bone epiphyses. – *Zoological Journal of the Linnean Society* **123**: 163–178.

Ciampaglio, C. N. 2002. Determining the role that ecological and developmental constraints play in controlling disparity: examples from the crinoid and blastozoan fossil record. – *Evolution & Development* **4**: 170–188.

Clemente-Carvalho, R.B., Antoniazzi, M.M., Jared, C., Haddad, C. F., Alves, A.C., Rocha, H.S., Pereira, G.R., Oliveira, D.F., Lopes, R.T. and Dos Reis, S.F. 2009. Hyperossificationin miniaturized toadlets of the genus *Brachycephalus* (Amphibia: Anura: Brachycephalidae): microscopic structure and macroscopic patterns of variation. – *Journal of Morphology* **270**: 1285–1295.

Djorović, A. and Kalezić, M. L. 2000. Paedogenesis in European newts (*Triturus*: Salamandridae): cranial morphology during ontogeny. – *Journal of Morphology* **243**: 229–232.

Dryden, I. L. and Mardia, K. V. 1998. Statistical Shape Analysis. John wiley and Sons, Chichester.

Duellman, W. E. and Trueb, L. 1986. Biology of Amphibians. McGraw-Hill, New York.

Ecker, A. 1889. The Anatomy of the Frog. A. Asher & Co., Amsterdam.

Fabrezi, M. 1992. El carpo de anuros. – *Alytes* **10**: 1–36.

Fabrezi, M. and Alberch, P. 1996. The carpal elements of anurans. – *Herpetologica* **52**: 188–204.

Frost, D. R. 2011. Amphibian Species of the World: an Online Reference. Version 5.5 (31 January, 2011). Electronic Database accessible at http://research.amnh.org/vz/herpetology/amphibia/American Museum of Natural History, New York, USA.

Giori, N. J., Beaupré, G. S. and Carter, D. R. 1993. Cellular shape and pressure may mediate mechanical control of tissue composition in tendons. – *Journal of Orthopedic Research* **11**: 581–591.

Gosner, K. L. 1960. A simplified table for staging anurans embryos and larvae with notes on identification. – *Herpetologica* **16**: 183–190.

Haas, A. 1999. Larval and metamorphic skeletal development in the fast-developing frog *Pyxicephalus adspersus* (Anura, Ranidae). – *Zoomorphology* **119**: 23–35.

Hanken, J. 1993. Adaptation of bone growth to miniaturization of body size. In: Hall, B. K. (Ed.) Bone Growth, pp. 79–104. CRC Press, Boca Raton, FL.

Hanken, J. and Hall, B. K. 1984. Variation and timing of the cranial ossification sequence of the Oriental firen bellied toad, *Bombina orientalis* (Amphibia, Discoglossidae). – *Journal of Morphology* **182**: 245–255.

Hanken, J. and Hall, B. K 1988. Skull development during anuran metamorphosis: I. Early development of the first three bones to form—the exoccipital, the parasphenoid, and the frontoparietal. – *Journal of Morphology* **195**: 247–256.

Hanken, J. and Hall, B. K. 1993. The Skull, vol. 2, p. 580. University of Chicago press, Chicago.

Havens, S. B. 2010. The role of skeletal in body size evolution of two North American frogs. Thesis Presented to the Faculty of the Graduate School of the Missouri University of Science and Technology.

Heyer, W. R. 1978. Systematics of the *fuscus* group of the genus *Leptodactylus* (Amphibia, Leptodactylidae). – *Contribution in Science, Natural History Museum, Los Angeles County* **29**: 1–85.

Ivanović, A., Vukov, T. D., Džukić, G., Tomaševič, N. and Kalezić, M. L. 2007. Ontogeny of skull size and shape changes within a framework of biphasic lifestyle: a case study in six *Triturus* species (Amphibia, Salamandridae). – *Zoomorphology* **126**: 173–183.

Kim, H. T., Olson, W. M. and Hall, B. K. 2009. Effects of hind limb denervation on the development of appendicular ossicles in the dwarf African clawed frog, *Hymenochirusboettgeri* (Anura: Pipidae). – *Acta Zoologica* **90**: 352–358.

Larson, P. M. 2002. Chondrocranial development in larval *Rana sylvatica* (Anura: Ranidae): a morphometric analysis of cranial allometry and ontogenetic shape change. – *Journal of Morphology* **252**: 131–144.

Larson, P. M. 2005. Ontogeny, phylogeny, and morphology in anuran larvae: morphometric analysis of cranial development and evolution in *Rana* tadpoles (Anura: Ranidae). – *Journal of Morphology* **264**: 34–52.

Larson, P. M. and de Sá, R.O. 1998. Chondrocranial morphology of *Leptodactylus* larvae (Leptodactylidae, Leptodactylinae): Its utility in phylogenetic reconstruction. – *Journal of Morphology* **238**: 287–305.

Le Minor, J. M. 1987. Comparative anatomy and significance of the sesamoid bone of the peroneus longus muscle (osperoneum). – *Journal of Anatomy* **151**: 85–99.

Lebedkina, N. S. 2004. Evolution of the amphibian skull. In: Kuzmin, S. L. (Ed.): Advances in Amphibian Research in the Former Soviet Union, pp. 1–239. Pensoft Publishers, Sofia.

Maglia, A. M. and Púgener, L. A. 1998. Skeletal development and adult osteology of *Bombina orientalis*(Anura: Bombinatoridae). – *Herpetologica* **54**: 334–363.

Maglia, A. M., Púgener, L. A. and Mueller, J. M. 2007. Skeletal morphology and postmetamorphic ontogeny of *Acris crepitans* (Anura: Hylidae): a case of miniaturization in frogs. – *Journal of Morphology* **268**: 194–223.

Mitteroecker, P., Gunz, P. and Bookstein, F. L. 2005. Heterochrony and geometric morphometric: a comparison of cranial growth in *Pan paniscus* versus *Pan troglodytes*. – *Evolution and Development* **7**: 244–258.

Nieuwkoop, P. D. and Faber, J. 1956. *Normal Table of Xenopus laevis (Daudin). A Systematical and Chronological Survey of the Development from Fertilized Egg till the End of Metamorphosis*. North-Holland Publ. Co., Amsterdam.

Perotti, M. G. 2001. Skeletal development of *Leptodactylus chaquensis* (Anura-Leptodactylidae). – *Herpetologica* **57**: 318–335.

Pisano, A., Rengel, D. and Lavilla, E. O 1993. Le nid souterrain comme chambre nuptiale pour un amphibien de Argentine. – *Revue Française Aquariol* **19**: 125–126.

Ponssa, M. L. 2006. On the osteology of a distinctive species of the genus *Leptodactylus: Leptodactylus laticeps* (Boulenger, 1917) (Anura, Leptodactylidae). – *Zootaxa* **1188**: 23–36.

Ponssa, M. L. 2008. Cladistic analysis and osteological descriptions of the frog species in the *Leptodactylus fuscus* species group (Anura, Leptodactylidae). – *Journal of Zoological Systematic and Evolutionary Research* **46**: 249–266.

Ponssa, M. L. and Heyer, W. R. 2007. Osteological characterization of four putative species of the genus *Adenomera* (Anura: Leptodactylidae), with comments on intra- and interspecific variation. – *Zootaxa* **1403**: 37–54.

Ponssa, M. L. and Vera Candioti, M. F. 2012. Patterns of skull development in anurans: size and shape relationship during post-metamorphic cranial ontogeny in five species of the *Leptodactylus fuscus* Group (Anura: Leptodactylidae). – *Zoomorphology* **131**: 349–362.

Ponssa, M. L., Goldberg, J. and Abdala, V. 2010a. Sesamoids in anurans: new data, old issues. – *The Anatomical Record* **293**: 1646–1668.

Ponssa, M. L., Jowers, M. J. and de Sá, R.O. 2010b. Osteology, natural history notes, and phylogenetic relationships of the poorly known Caribbean frog *Leptodactylus nesiotus*(Anura, Leptodactylidae). – *Zootaxa* **2646**: 1–25.

Ponssa, M. L., Brusquetti, F. and Souza, F. L. 2011. Osteology and intraspecific variation of *Leptodactylus podicipinus* (Anura: Leptodactylidae), with comments on the relationship between osteology and reproductive modes. – *Journal of Herpetology* **45**: 79–93.

Púgener, L. A. and Maglia, A. M. 1997. Osteology and skeletal development of *Discoglossus sardus*(Anura: Discoglossidae). – *Journal of Morphology* **233**: 267–286.

Reading, C. J. and Jofré, G. M. 2003. Reproduction in the nest building vizcacheras frog *Leptodactylus bufonius* in central Argentina. – *Amphibia-Reptilia* **24**: 415–427.

Rohlf, F. J. 2003. tpsRelw, Relative Warps Analysis, version 1.37, Available at: http://life.bio.sunysb.edu/morph/morphmet.html.

Rohlf, F. J. 2010. TpsDig Program Version 2.16. Ecology and evolution, SUNY at Stony Brook.

de Sá, R.O. 1988. Chondrocranium and ossification sequence of *Hyla lanciformis*. – *Journal of Morphology* **195**: 345–355.

de Sá, R. O. and Lavilla, E. O. 1996. Características de la osificación craneal en *Phyllomedusa boliviana* (Anura: Hylidae). – *Cuadernos de Herpetología* **9**: 69–73.

de Sá, R.O. and Trueb, L. 1991. Osteology, skeletal development, and chondrocranial structure of *Hamptophryne boliviana* (Anura: Microhylidae). – *Journal of Morphology* **209**: 311–330.

de Sá, R.O., Brandão, R. and Guimarães, L. D. 2007. Description of the tadpole of *Leptodactylus pustulatus* Peters, 1870 (Anura: Leptodactylidae). – *Zootaxa* **1523**: 49–58.

Sarin, V. K., Erickson, G. M. and Giori, N. J. 1999. Coincident development of sesamoid bones and clues to their evolution. – *Anatomical Record* **257**: 174–180.

Sheil, C. A. 1999. Osteology and skeletal development of *Pyxicephalus adspersus*(Anura: Ranidae: Ranimae). – *Journal of Morphology* **240**: 49–75.

Sheil, C. A. and Alamillo, H. 2005. Osteology and skeletal development of *Phyllomedusa vaillanti* (Anura: Hylidae: Phyllomedusinae) and a comparison of this arboreal species with a terrestrial member of the genus. – *Journal of Morphology* **265**: 343–368.

Shofner, W. P. Jr. 1983. The post-metamorphic development of the peripheral auditory system of the bullfrog, *Rana catesbeiana*: an anatomical and physiological study. PhD Thesis. University of Illinois at Urbana-Champaign, p. 184.

Smit, A. L. 1953. The ontogenesis of the vertebral column of *Xenopus laevis* (Daudin) with special reference to the segmentation of the metotic region of the skull. *Annals of the University of Stellenbosch* **29**: 79–136.

Trewavas, E. 1933. The hyoid and larynx of the Anura. – *Philosophical Transactions of the Royal Society of London* **222**: 401–527.

Trueb, L. 1973. Bones, frogs, and evolution. In: Vial, J. L. (Ed.): Evolutionary Biology of the Anurans: Contemporary Research on Major Problems, pp. 65–132. University of Missouri Press, Columbia.

Trueb, L. 1985. A summary of osteocranial development in anurans with notes on the sequence of cranial ossification in *Rhinophrynus dorsalis*(Anura: Pipoidea: Rhinophrynidae). – *South African Journal of Science* **81**: 181–185.

Trueb, L. 1993. Patterns of cranial diversity within the Lissamphibia. In: Hanken, J. J. and Hall, B. K. (Eds): The Skull. Patterns of Structural and Systematic Diversity, Vol. 2, pp. 255–343. The University of Chicago Press, Chicago.

Trueb, L. and Hanken, J. 1992. Skeletal development in *Xenopus laevis*(Anura: Pipidae). – *Journal of Morphology* **214**: l–41.

Trueb, L., Púgener, L. A. and Maglia, A. M. 2000. Ontogeny of the bizarre: an osteological description of *Pipa pipa* (Anura: Pipidae), with an account of skeletal development in the species. – *Journal of Morphology* **243**: 75–104.

Vera Candioti, M. F., Brusquetti, F. and Netto, F. 2007. Morphological characterization of *Leptodactylus elenae* tadpoles (Anura: Leptodactylidae: *L. fuscus* group), from central Paraguay. – *Zootaxa* **1435**: 1–17.

Vickaryous, M. K. and Olson, W. M. 2007. Sesamoids and Ossicles in the Appendicular Skeleton. In: Hall, B. K. (Ed.): Fins Into Limbs: Evolution, Development, and Transformation, pp. 323–341. University of Chicago Press, Chicago.

Wassersug, R. J. 1976. A procedure for differential staining of cartilage and bone in whole formalin-fixed vertebrates. – *Staining Technique* **51**: 131–134.

Wassersug, R. J. and Sperry, D. G. 1997. The relationship of locomotion to differential predation on *Pseudacris triseriata* (Anura, Hylidae). – *Ecology* **58**: 830–839.

Wiens, J. J. 1989. Ontogeny of the skeleton of *Spea bombifrons* (Anura: Pelobatidae). –*Journal of Morphology* **202**: 29–51.

Wild, E. R. 1997. Description of the adult skeleton and developmental osteology of the hyperossified horned frog, *Cerathrophys cornuta* (Anura, Leptodactylidae). – *Journal of Morphology* **232**: 169–206.

Wild, E. R. 1999. Description of the chondrocranium and osteogenesis of the chacoan burrowing frog, *Chacophrys pierottii* (Anura: Leptodactylidae). – *Journal of Morphology* **242**: 229–246.